

Many-field Inflation: Universality or Prior Dependence?

Perseas Christodoulidis,¹ Diederik Roest,¹ and Robert Rosati²

¹*Van Swinderen Institute for Particle Physics and Gravity,
University of Groningen, Nijenborgh 4, 9747 AG Groningen, The Netherlands*

²*Theory Group, Department of Physics, University of Texas at Austin, Austin, TX 78712, USA*

We investigate the observational signatures of many-field inflation and present analytic expressions for the spectral index as a function of the prior. For a given prior we employ the central limit theorem and the horizon crossing approximation to derive universal predictions, as found previously. However, we also find a specific dependence on the prior choice for initial conditions that has not been seen in previous studies. Our main focus is on quadratic inflation, for which the initial conditions statistics decouple from those of the mass distribution, while other monomials are also briefly discussed. We verify the validity of our calculations by comparing to full numerical simulations with 10^2 fields using the transport method.

Introduction – Inflation is the leading paradigm for the generation of primordial perturbations that seeded structure formation. The latest *Planck* results confirm the generic traits of this paradigm and are compatible with the simplest models of single field slow-roll inflation [1]. In such models, the dissipative nature of inflationary dynamics reduces the order of the scalar-field equation from second to first providing a notion of initial conditions independence [2, 3]. This leads to specific predictions for cosmological observables, e.g. the scalar spectral index, its running and the tensor-to-scalar ratio. For the simplest model, quadratic inflation, these are given by $n_s = 1 - 2/N_*$, $\alpha_s = -2/N_*^2$ and $r = 8/N_*$, where N_* corresponds to the CMB horizon crossing moment.

Though CMB data are well described by the predictions of single-field inflation, UV-complete theories naturally predict many light scalar fields to be present in the early universe. A natural question then concerns the generalization of single-field observables to multiple fields with a non-trivial potential $V(\Phi_i)$ with $i = 1, \dots, N_f$ and a Cartesian metric on field space. While complicated in general, analytic control can be achieved in the slow-roll slow-turn limit with (again neglecting the acceleration)

$$\sqrt{3V}\dot{\Phi}_i + V_i \approx 0. \quad (1)$$

However, in this approximation background dynamics is not determined uniquely¹. Instead, Eqs. (1) yields an N_f -dimensional hypersurface in $2N_f$ -dimensional phase space and therefore there is an $(N_f - 1)$ -dimensional hypersurface that represents CMB horizon crossing. This results in an intrinsic dependence of the observables on the initial conditions, even in the slow-roll limit.

Turning to perturbations, analytical expressions for an arbitrary number of fields exist in the horizon-crossing

approximation² [5–8]. This method takes into account superhorizon evolution of curvature perturbation but ignores contributions from the fields’ position at the end of inflation. Moreover, it assumes the slow-roll approximation and an analytic expression of N_e in terms of the fields, and thus its applicability is more limited. On the contrary, the standard numerical approach is by means of the transport method [10–15] which solves the perturbations’ equations of motion equivalent to tree level in the in-in formalism, and requires no slow-roll or horizon crossing approximations.

A simple and well-studied multi-field model is N-flation, consisting of a sum of quadratic potentials [16, 17]. Early investigations relied on the horizon crossing approximation which allows for simple calculation of the spectral index, tensor to scalar ratio, running and non-gaussianity. More specifically, r is found independent of initial conditions and the number of fields [18], whereas the spectral index and its running inherits the dependence on initial conditions [19, 20].

N-flation has received interest in the axion landscape community, see e.g. [21–23], because it can approximate inflation towards a cosine minimum. These models can make universal landscape predictions based in part on the universality of N-flation [24]. A similar predictivity has been found in recent many-field numerical investigations in other contexts [14, 15, 25, 26]. It is the goal of this paper to elucidate these simple predictions of many-field models and investigate their prior dependence.

Many-field N-flation – For N-flation, $V = \frac{1}{2} \sum m_i^2 \Phi_i^2$, the spectral index can be calculated by the fields’ values at horizon crossing, which satisfy the hypersphere constraint $\sum \Phi_{i,*}^2 = 4N_*$ (star quantities are evaluated at horizon crossing). If evolution has started at

¹ This can be contrasted with recently discovered models in which the interplay between the potential and field-metric can lead to one-parameter “single-field” trajectories [4].

² Although called horizon crossing approximation it does not evaluate the power spectra at horizon crossing but rather expresses every observable at the end of inflation using their values at horizon crossing [9].

an earlier number of e-folds their values at horizon crossing will be related to the initial displacements through the slow-roll equations of motion (1)

$$\Phi_{i,*} = \Phi_i e^{-m_i^2 \tau_*}, \quad (2)$$

where Φ_i are the initial field displacements with $\sum \Phi_i^2 = 4N_0$. The new time variable is defined by $dN = -V d\tau$ and ranges from $\tau = 0$ to τ_* during $N = N_0$ to N_* (the e-folding number runs backwards).

The previous sums can be rewritten in a convenient way by introducing the *sample average* $\sum A_i \equiv N_f \langle A \rangle_s$. This quantity is in general not equal to the *expectation value* $\langle A \rangle$; only when the conditions of the central limit theorem are satisfied the two coincide at $N_f \rightarrow \infty$. In our problem, expectation values correspond to double integrals

$$\langle \phi^k (m^2)^l \rangle = \int d\phi d(m^2) (m^2)^l \phi^k P(\phi, m^2), \quad (3)$$

where $P(\phi, m^2)$ is the joint distribution of fields and masses. When the two random variables are independent, the probability distribution becomes product-separable and the average value splits to product of averages $\langle \phi^k (m^2)^l \rangle = \langle \phi^k \rangle \langle (m^2)^l \rangle$.

Rescaling the initial values of the fields $\Phi_i = 2\sqrt{N_0/N_f} \phi_i$ their sample average becomes equal to $\langle \phi^2 \rangle_s = 1$. Thus, the spectral index at horizon crossing in this notation is given by

$$n_s = 1 - \frac{1}{N_*} \left(1 + \frac{\langle e^{-2m^2 \tau_*} \phi^2 \rangle_s \langle m^4 e^{-2m^2 \tau_*} \phi^2 \rangle_s}{\langle m^2 e^{-2m^2 \tau_*} \phi^2 \rangle_s^2} \right), \quad (4)$$

where the sample averages are calculated for a specific realization of the fields and the masses and we used $N_0 \langle e^{-2m^2 \tau_*} \phi^2 \rangle_s = N_*$. For a choice of masses (drawn from a given mass distribution) the numerical value of the previous equation depends on the fields' realization, leading to an intrinsic initial conditions dependence³. In the following we will discuss two physically well-motivated priors that have been considered in the literature, the number of e-folds N_0 [9] and energy prior E_0 [27] and examine how time evolution affects predictions. For these two priors the distribution $P(\phi)$ is not necessary for calculation of $\langle n_s \rangle$ since the field- or energy-dependent terms decouple from masses.

N_0 -prior: Every vector $\vec{\phi}$ corresponds to a point of the N_f -dimensional hypersphere with radius 1. The method to obtain a random point includes sampling from the multi-variate distribution $\mathcal{N}(0, 1)$ and then dividing by

³ It can be shown that n_s is strictly bounded $n_s \in [n_{s,min}, 1 - 2/N_*]$, with the lower bound corresponding to a configuration where only the heaviest and lightest fields are non-zero and contribute with equal energies.

the norm of the vector. Assuming that the ϕ_i 's are uncorrelated with the masses (including the time dependent term $e^{-2\lambda_i \tau_*}$) and employing similar techniques as [25], one can show that at the limit of infinite number of fields the ratio in Eq. (4) is normally distributed with mean

$$\frac{1}{N_*} \frac{\langle e^{-2m^2 \tau_*} \rangle \langle m^4 e^{-2m^2 \tau_*} \rangle}{\langle m^2 e^{-2m^2 \tau_*} \rangle^2}, \quad (5)$$

and standard deviation that scales as $1/\sqrt{N_f}$; thus, we expect sharp many-field predictions. The expectation values are integrals over the mass distribution that should be evaluated at τ_* , the latter given as a solution of the integral equation

$$\langle e^{-2m^2 \tau_*} \rangle \equiv \int dm^2 P(m^2) e^{-2m^2 \tau_*} = \frac{N_*}{N_0}. \quad (6)$$

Thus, this choice of prior results in a spectral index that is given by a specific time-dependent combination of the moments of the mass distribution: at $\tau = 0$, i.e. starting at a random point on N_* , this is given by the variance of the distribution, while starting at a random point at a higher N_0 there will also be higher-order moments that contribute.

E_0 -prior: Instead one can start with a fixed initial energy E_0 , and assume the energy per field to be uncorrelated with the mass distribution. Defining initial energies as $2E_i = m_i^2 \phi_i^2$ its sample average is $\langle E \rangle = E_0/(4N_0)$. The central limit theorem implies that, at large N_f , the ratio in (4) becomes

$$\frac{1}{N_*} \frac{\langle m^{-2} e^{-2m^2 \tau_*} \rangle \langle m^2 e^{-2m^2 \tau_*} \rangle}{\langle e^{-2m^2 \tau_*} \rangle^2}. \quad (7)$$

The initial energy and the number of e-folds are related by $E_0 = 2N_0/\langle m^{-2} \rangle$ while τ_* is calculated by Eq. (6). Hence, for this initial conditions prior, the spectral index is given by a different time-dependent combination of the moments of $P(m^2)$.

The asymptotic behaviour (for either prior) can be inferred as follows: for sufficiently large time $\tau_* \gg 1$ if the lightest field is non-zero it will dominate the numerator and denominator in Eq. (4) and the ratio asymptotes to $\langle e^{-2m^2 \tau_*} \rangle_s / \langle \phi_1^2 e^{-2m_1^2 \tau_*} \rangle$. Using Eq. (6) this term is equal to 1 and so $n_s \rightarrow 1 - 2/N_*$, the single field result. On the contrary, if the mass distribution is gapless (i.e. the lightest field is massless) the previous ratio becomes undefined and the asymptotic value only depends on the behavior of the mass spectrum around the massless point. Precisely, for a mass spectrum with lowest order term $P(\lambda) \propto \lambda^\alpha + \mathcal{O}(\lambda^{1+\alpha})$, the asymptotic value is given by

$$n_s \xrightarrow{N_0 \rightarrow \infty} 1 - \frac{1}{N_*} \left(2 + \frac{1}{\gamma + \alpha} \right), \quad (8)$$

where $\gamma = 1$ for the N_0 -prior, $\gamma = 0$ for the E_0 -prior and $\gamma + \alpha > 0$.

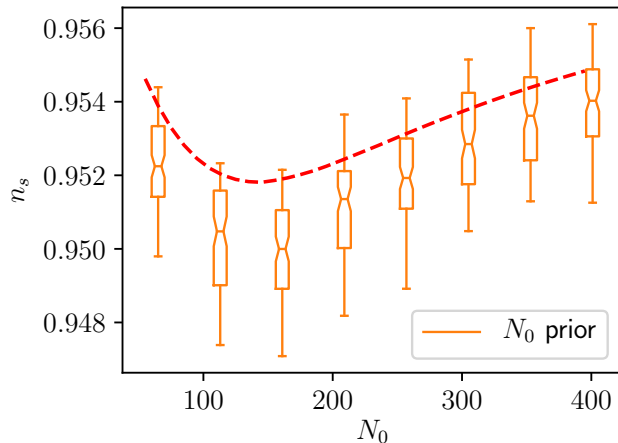


FIG. 1. Transport method simulations of 100-field N -flation with initial conditions set to a fixed radius (i.e. a fixed number of e -folds) and masses drawn from the Marcenko-Pastur distribution with $\beta = 1/2$. We compare the transport method (orange) and our analytic result (dashed, red) for initial conditions drawn uniformly over the hypersphere. At each radius, the numeric data are binned into a box and whiskers marking the 50% and 95% confidence intervals respectively. Agreement is at the per mil level.

Finally, the above formalism allows for a straightforward calculation of the running, by deriving Eq. (4) w.r.t. N_* . This results again in specific combinations of the (time-dependent) averages $q_k \equiv \langle e^{-2m^2\tau_*} m^k \phi^2 \rangle$

$$\alpha_s = \frac{1}{N_*^2 q_2^3} (q_2^3 + 2q_0 q_2 q_4^2 - q_0^2 q_6), \quad (9)$$

at lowest order in slow-roll.

Numerical results – The above approximations and trends are confirmed by full numerical simulations. We use the `Inflation.jl` transport code⁴, which is capable of solving the perturbations' equations of motion for $N_f \sim 100$ using the transport method. We take the mass distribution to be Marcenko-Pastur [20]

$$p(\lambda) = \frac{1}{2\pi\lambda\beta\sigma^2} \sqrt{(b-\lambda)(\lambda-a)} \quad (10)$$

where $a = \sigma^2(1 - \sqrt{\beta})^2$ and $b = \sigma^2(1 + \sqrt{\beta})^2$. The overall normalization σ^2 drops out of the spectral index, and β sets the width of the distribution. With these mass distributions and a horizon crossing surface at $N_* = 55$, we have taken 100 samples per prior and plotted the spectral index in Figs. 1- 3 and 5.

⁴ The code is written in Python and Julia and will be publicly available soon.

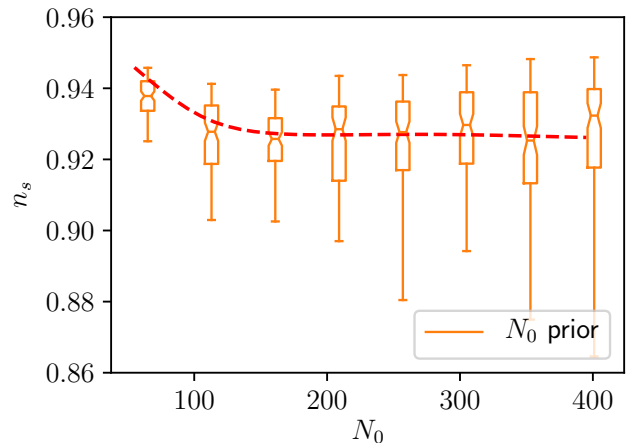


FIG. 2. Transport method simulations of 100-field N -flation with initial conditions set to a fixed radius (i.e. a fixed number of e -folds) and masses drawn from the Marcenko-Pastur distribution with $\beta = 1$ (a gapless spectrum). We compare the transport method (orange) and our analytic result (dashed, red) for initial conditions drawn uniformly over the hypersphere. At each radius, the data are binned as in Fig. 1. Agreement is at the per mil level.

There are a number of striking results that follow from our general analysis. First of all, for a given initial hypersphere of the N_0 -prior, the probability distribution has a clear peak in the many-field limit. Secondly, this peak value depends on the radius of the initial hypersphere. The peaked distribution was already found in [24] but not the dependence on the initial hypersurface. Instead, we see a clear trend: starting at $N_0 = 55$ the spectral index set by the variance of the mass distribution, the peak value first goes down and reaches a minimum around $N_0 \sim 160$ for the specific mass distribution of Fig. 1. Starting at yet larger radii, the heavier fields have more time to decay and this will eventually result in a single-field prediction in the large N_0 limit.

The presence of a minimum in $n_s(N_0)$ (i.e., a minimum of n_s at some initial radius N_0 with $N_* < N_0 < \infty$) can be estimated by requiring that $n_s(N_*)$ is lower than its asymptotic value and $dn_s/d\tau|_{\tau=\tau_*} < 0$. For a mass distribution with $\langle m^2 \rangle = 1$ and an asymptotic relation $n_s \rightarrow 1 - c/N_*$, these conditions imply a minimum will occur whenever $\langle m^4 \rangle > c - 1$ and $\langle m^6 \rangle < 2c(c - 1)$. For Marcenko-Pastur, the expectation values for the quartic and sextic moments are given by $1 + \beta$ and $1 + 3\beta + \beta^2$, respectively. The gapped case that we consider has $\beta = 1/2$ and asymptotes to $c = 2$ and therefore satisfies both conditions, leading to a minimum at the (N_0, n_s) plot.

Next, we examine the gapless Marcenko-Pastur distribution with $\beta = 1$ in Fig. 2 for the N_0 -prior. Instead of converging to the single-field result, we instead find $n_s \rightarrow 1 - 4/N_* \sim 0.927$. This asymptotic value only depends on the behavior of the mass spectrum around the

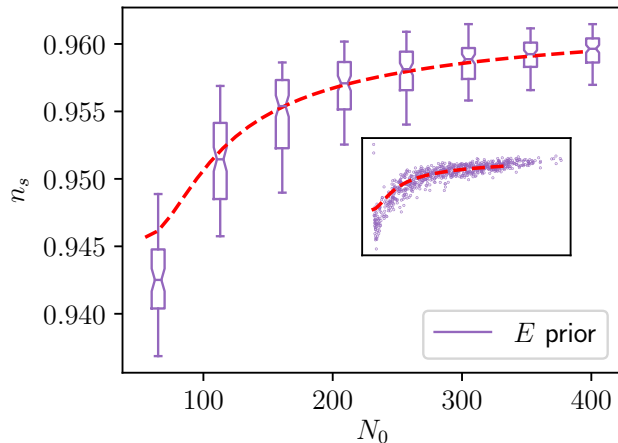


FIG. 3. Transport method simulations of 100-field N -flation with initial conditions set to a fixed energy (i.e. constrained to a hyper-ellipse) and masses drawn from the Marcenko-Pastur distribution with $\beta = 1/2$. The data are binned by the number of e -folds an equipartitioned-energy initial condition would have at the same energy, over a range of energies. The number of e -folds varies by as much as $\pm 30\%$ from equipartitioned energies. At each energy, the data are binned into a box similarly to Fig 1, or alternatively the unbinned data are displayed in the inset. The dashed red line marks our corresponding many-field analytic result. Agreement is at least at the per mil level.

massless point $p(m^2) \sim m^{-1}$, in accordance to the discussion in the previous section. Due to the lower asymptotic value, no minimum occurs.

Finally, we examine the E_0 -prior, which corresponds to selecting random field values that have a fixed energy, forming a hyper-ellipse. When starting at CMB horizon crossing, this will lead to the spectral index determined by the moments $\langle m^{-2} \rangle$, $\langle m^2 \rangle$. For higher energies the resulting spectral index at CMB horizon crossing can be easily calculated from the time-dependent moments, and is illustrated in Fig. 3. We provide a similar numerical analysis that confirms the trend in this evolution.

Higher monomials – For higher monomials with $V = \frac{1}{n} \sum \lambda_i \Phi_i^n$ the number of e -folds as a function of the fields is given by $\sum \Phi_i^2 = 2nN_0$. The slow-roll equations (1) imply

$$\Phi_{i,*} = (\Phi_i^{2-n} + (n-2)\lambda_i \tau_*^2)^{\frac{1}{2-n}}, \quad (11)$$

where τ has field dimensions for $n \neq 2$. Using e.g. the N_0 -prior introducing normalised fields $\Phi_i = 2n\sqrt{N_0/N_f}\phi_i$ and the rescaled time $\xi = \tau(2nN_0/N_f)^{n/2-1}$, the moment of CMB horizon crossing is given by

$$\langle (\phi_i^{2-n} + (n-2)\lambda\xi_*^2)^{\frac{2}{2-n}} \rangle_s = \frac{N_*}{N_0}. \quad (12)$$

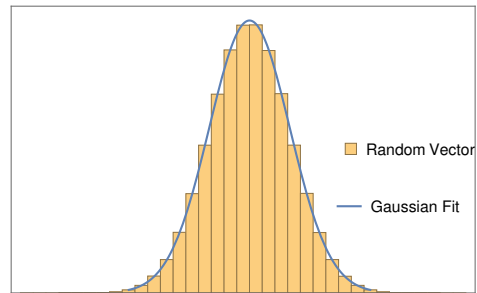


FIG. 4. Probability density of the components of a random vector for $N_f = 10^7$ and the corresponding analytically estimated Gaussian distribution. Agreement is perfect.

The horizon crossing formula is similarly

$$n_s = 1 - \frac{1}{N_*} - \frac{n}{2N_0} \frac{\langle \lambda^2 (\phi_i^{2-n} + (n-2)\lambda\xi_*^2)^{\frac{2n-2}{2-n}} \rangle_s}{\langle \lambda (\phi_i^{2-n} + (n-2)\lambda\xi_*^2)^{\frac{2n-2}{2-n}} \rangle_s^2}. \quad (13)$$

For $N_f \rightarrow \infty$ sample averages can be calculated from expectation values if the distribution of ϕ_i is known.

Because of the hypersphere constraint, the distribution $P(\Phi)$ is not a Gaussian for finite N_f (for instance, the distribution for one field is a sum of two delta's located at ± 1). However, when $N_f \rightarrow \infty$ the distribution $P(\Phi)$, which can be seen as the distribution of components of a random vector on the N -sphere, asymptotes to a Gaussian distribution with zero mean and standard deviation $1/\sqrt{N_f}$. For the rescaled fields ϕ their statistical moments⁵ for $N_f \rightarrow \infty$ can be reproduced by the expectation values $\langle \phi^n \rangle$ using $P(\phi) = e^{-\phi^2/2}/\sqrt{2\pi}$. With the distribution of the fields known, expectation values correspond to double integrals over fields and 'masses' λ .

In Fig. 5 we depict numerical simulations for quartic fields using the N_0 -prior. In contrast to the quadratic case, there is no minimum, since the conditions for its existence are not satisfied, and instead we observe a monotonic increase towards the asymptotic value. The horizon crossing formula is again in a good agreement with the numerical results.

Discussion – In this paper we have examined inflationary observables of sum-separable monomial potentials in the horizon crossing approximation and provided elegant analytical expressions. Although for a chosen prior there are in principle infinite different field and mass realizations (parameterized as random variables), the computed distribution of observables in the many-field limit has a sharp peak. This universality can be attributed to the central limit theorem since the analytical formulae include sums of random variables.

⁵ These can be calculated independently as integrals over the N_f -sphere $\langle \psi_i^n \rangle = \int d\Omega \psi_i^n / \int d\Omega$, expressing fields in spherical coordinates.

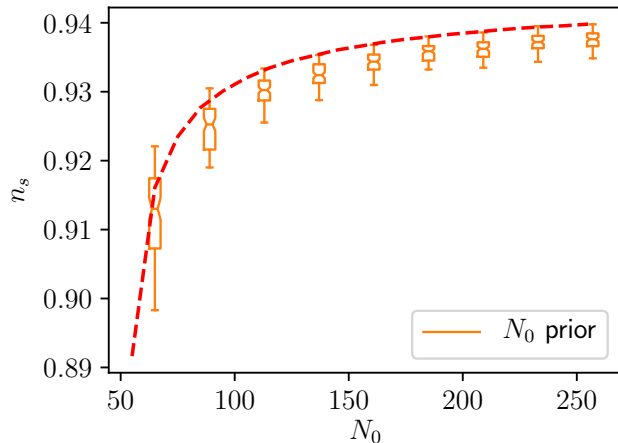


FIG. 5. *Transport method simulations of 100-field quartic monomial inflation with initial conditions set to a fixed radius (i.e. a fixed number of e -folds) and ‘masses’ drawn from the Marcenko-Pastur distribution with $\beta = 1/2$. Agreement is at the per mil level.*

This universality is offset, however, by a strong dependence on the prior and the mass distribution. Different priors, as seen in Figs 1-3, can lead to different predictions, both in the spectral index and its running. Specifically, for a gapped mass spectrum, the predictions range from variance-dominated to the single-field limit. Instead, for gapless mass distributions, the behaviour of the probability distribution for the lightest masses strongly determines its asymptotic behavior at high N_0 , as seen in Fig. 2.

In the absence of a non-trivial scalar-field geometry, observables derived for quadratic potentials can be seen as generic: the large- N_f limit pushes the horizon crossing point towards the minimum in field space, where more complicated models can be approximated with a quadratic potential. This suggests that the universality and prior dependence identified in this paper should apply to a range of more general models as well. It would be interesting to investigate the scope of our results in this direction, as well as to investigate the effects of scalar geometry in the many-field limit.

Acknowledgments – It is a pleasure to thank Jonathan Frazer, Mafalda Dias and John Stout for valuable discussions at the first stages of this project. We would also like to thank Oliver Janssen for useful discussions. PC and DR acknowledge support from the Dutch Organisation for Scientific Research (NWO). RR was supported by the U.S. National Science Foundation under Grant PHY-1620610.

- [1] Y. Akrami *et al.* [Planck Collaboration], “Planck 2018 results. X. Constraints on inflation,” arXiv:1807.06211 [astro-ph.CO].
- [2] D. S. Salopek and J. R. Bond, Phys. Rev. D **42**, 3936 (1990).
- [3] A. R. Liddle, P. Parsons and J. D. Barrow, Phys. Rev. D **50**, 7222 (1994) [astro-ph/9408015].
- [4] P. Christodoulidis, D. Roest and E. I. Sfakianakis, arXiv:1903.03513 [gr-qc].
- [5] A. A. Starobinsky, JETP Lett. **42**, 152 (1985) [Pisma Zh. Eksp. Teor. Fiz. **42**, 124 (1985)].
- [6] M. Sasaki and E. D. Stewart, Prog. Theor. Phys. **95**, 71 (1996) [astro-ph/9507001].
- [7] F. Vernizzi and D. Wands, JCAP **0605**, 019 (2006) [astro-ph/0603799].
- [8] S. A. Kim and A. R. Liddle, Phys. Rev. D **74**, 063522 (2006) [astro-ph/0608186].
- [9] J. Frazer, JCAP **1401**, 028 (2014) [arXiv:1303.3611 [astro-ph.CO]].
- [10] M. Dias, J. Frazer and D. Seery, JCAP **1512**, no. 12, 030 (2015) doi:10.1088/1475-7516/2015/12/030 [arXiv:1502.03125 [astro-ph.CO]].
- [11] D. Seery, D. J. Mulryne, J. Frazer and R. H. Ribeiro, JCAP **1209**, 010 (2012) doi:10.1088/1475-7516/2012/09/010 [arXiv:1203.2635 [astro-ph.CO]].
- [12] D. J. Mulryne, D. Seery and D. Wesley, JCAP **1104**, 030 (2011) doi:10.1088/1475-7516/2011/04/030 [arXiv:1008.3159 [astro-ph.CO]].
- [13] S. Paban and R. Rosati, JCAP **1809**, no. 09, 042 (2018) doi:10.1088/1475-7516/2018/09/042 [arXiv:1807.07654 [astro-ph.CO]].
- [14] M. Dias, J. Frazer and M. c. D. Marsh, JCAP **1801**, no. 01, 036 (2018) [arXiv:1706.03774 [astro-ph.CO]].
- [15] T. Bjorkmo and M. C. D. Marsh, JCAP **1802**, no. 02, 037 (2018) [arXiv:1709.10076 [astro-ph.CO]].
- [16] S. Dimopoulos, S. Kachru, J. McGreevy and J. G. Wacker, JCAP **0808**, 003 (2008) [hep-th/0507205].
- [17] Y. S. Piao, Phys. Rev. D **74**, 047302 (2006) [gr-qc/0606034].
- [18] L. Alabidi and D. H. Lyth, JCAP **0605**, 016 (2006) [astro-ph/0510441].
- [19] S. A. Kim and A. R. Liddle, Phys. Rev. D **74**, 023513 (2006) [astro-ph/0605604].
- [20] R. Easther and L. McAllister, JCAP **0605**, 018 (2006) [hep-th/0512102].
- [21] C. Long, L. McAllister and J. Stout, JHEP **1702**, 014 (2017) doi:10.1007/JHEP02(2017)014 [arXiv:1603.01259 [hep-th]].
- [22] T. C. Bachlechner, K. Eckerle, O. Janssen and M. Kleban, arXiv:1810.02822 [hep-th].
- [23] T. C. Bachlechner, K. Eckerle, O. Janssen and M. Kleban, arXiv:1902.05952 [hep-th].
- [24] R. Easther, J. Frazer, H. V. Peiris and L. C. Price, Phys. Rev. Lett. **112**, 161302 (2014) [arXiv:1312.4035 [astro-ph.CO]].
- [25] L. C. Price, H. V. Peiris, J. Frazer and R. Easther, Phys. Rev. Lett. **114**, no. 3, 031301 (2015) [arXiv:1409.2498 [astro-ph.CO]].
- [26] M. Dias, J. Frazer and M. C. D. Marsh, Phys. Rev. Lett. **117**, no. 14, 141303 (2016) [arXiv:1604.05970 [astro-ph.CO]].
- [27] R. Easther and L. C. Price, JCAP **1307**, 027 (2013) [arXiv:1304.4244 [astro-ph.CO]].